

## Investigation into the influence and mechanism of carbonated recycled fine powder on the performance of cement-based materials

Chen Denghai<sup>1,2</sup>, Li Ying<sup>1,2\*</sup>, Li Jiachen<sup>1,2</sup>, Zhao Gang<sup>1,2</sup>, Zhang Rui<sup>1,2</sup>

<sup>1</sup> School of Civil Engineering and Water Resources, Qinghai University, Xining 810016, Qinghai, China  
<sup>2</sup> Qinghai Province Key Laboratory of Building Energy-saving Materials and Engineering Safety, Xining 810016, Qinghai, China  
\* Corresponding author's e-mail: liying.qh@163.com

### ABSTRACT

Recycled fine powder is an important pathway for the resource utilization of construction and demolition waste; however, its low reactivity and the unstable influence on the performance of cement-based materials after incorporation remain critical barriers to large-scale application. Carbonation treatment not only enables CO<sub>2</sub> sequestration and provides environmental benefits but also improves the physicochemical properties of recycled fine powder. In this study, recycled fine powder was treated by a dry carbonation method and used to partially replace cement at substitution levels of 10%, 20%, and 30% to prepare mortar specimens. The effects of carbonated recycled fine powder on the macroscopic mechanical properties, early hydration heat evolution, and pore structure development of mortar were systematically investigated, with the aim of providing data support and theoretical basis for the optimized utilization of recycled fine powder in green and low-carbon construction materials. The results demonstrated that carbonation treatment generated CaCO<sub>3</sub>, which served as nucleation sites for secondary hydration of cement, thereby accelerating hydration, increasing heat release, refining pore structure, and enhancing mechanical performance. Compared with mortars containing uncarbonated recycled fine powder the 3-day compressive strength increased by 15.2%, 14.3%, and 8.0%, while the 28-day compressive strength showed little difference, indicating that carbonation primarily enhanced early-age strength. For flexural strength, the 28-day values increased by 9.7%, 4.0%, and 0.7%, consistent with the 3-day results. Pore structure analysis revealed that total porosity decreased by 0.43%, 0.45%, and 0.51%, while the cumulative heat release within 72 h increased by 0.8%, 9.4%, and 7.9%. These findings elucidate the mechanism by which carbonation treatment enhances early-age strength of mortar through promoting hydration reactions and improving pore structure.

**Keywords:** carbonation treatment, carbonated recycled fine powder, hydration characteristics, mass loss, micro-pore structure, recycled fine powder.

### INTRODUCTION

With the rapid advancement of urbanization and the continuous expansion of the construction industry in China, the annual generation of construction waste has been increasing, exerting a substantial burden on the ecological environment. The resource utilization of construction waste not only reduces landfilling and stockpiling but also conserves natural resources and mitigates environmental pollution, thereby offering significant economic and environmental benefits [1,2]. In

line with China's commitment to achieving carbon neutrality by 2060, carbon sequestration and emission reduction have become pressing issues across all sectors [3–5]. Due to its large scale and high energy consumption, the construction industry has long been a major contributor to global CO<sub>2</sub> emissions, accounting for approximately 30–40% annually [6,7]. Consequently, reducing carbon emissions in the construction sector represents a critical challenge for future sustainable development [5]. Against this background, the resource utilization of construction and demolition

waste not only alleviates the excessive exploitation of natural resources but also promotes the low-carbon transformation and green development of the construction industry [8–10].

At present, the resource utilization of construction and demolition waste (CDW) primarily includes recycled coarse aggregate, recycled fine aggregate, and a considerable amount of dust particles with a particle size of less than 0.075 mm generated during the recycling process, commonly referred to as recycled fine powder [11]. This recycled powder accounts for approximately 10–20% of the total CDW, and its main components consist of silica, hydrated products such as calcium hydroxide, and unhydrated tricalcium silicate [4]. Although it exhibits certain pozzolanic activity and is generally used as a supplementary cementitious material in cement-based systems, its relatively low reactivity has resulted in limited utilization [12–14]. Compared with recycled fine powder, research on recycled coarse aggregate has received greater attention. Several studies have employed recycled aggregates to prepare recycled concrete [15]. However, due to the substantial amount of residual cement mortar adhered to the surface of recycled aggregates, these aggregates exhibit high porosity and water absorption, which significantly reduce the compressive strength, permeability, and other durability properties of recycled aggregate concrete [16–19]. Hamed Dabiri reported that replacing natural coarse aggregate with recycled coarse aggregate (RCA) at substitution levels ranging from 10% to 100% led to notable changes in the primary mechanical properties of concrete. The experimental results showed that, compared with control concrete samples, the maximum compressive strength, flexural strength, splitting tensile strength, density, and slump decreased by 19.4%, 18.3%, 19.6%, 19.5%, and 25.0%, respectively [20]. To address the inherent drawbacks of RCA, such as high porosity and strong water absorption, several improvement methods have been proposed, including carbonation, mechanical grinding, immersion treatment, and mineral admixture activation. Among these, accelerated carbonation not only effectively enhances the physical and mechanical properties of RCA but also captures CO<sub>2</sub>, thereby contributing to emission reduction and promoting the low-carbon development of the construction industry [21–23]. Carbonation technology has also been widely applied to modify other recycled materials. For instance,

Veronica Viola investigated the carbonation potential of wood ash under different relative humidity, liquid-to-solid ratios, and temperature conditions. The results demonstrated that prolonged carbonation increased CaCO<sub>3</sub> production, decreased porosity, and improved the mechanical performance of samples with higher carbonate content [24]. Previous studies further revealed that carbonation of RCA generates CaCO<sub>3</sub>, which can fill aggregate pores and consequently enhance aggregate strength [25,26]. Hanxiong Lyu et al. incorporated carbonated glass powder as a partial replacement for ordinary Portland cement to prepare sustainable cement pastes. Their findings indicated that carbonated glass powder improved the sustainability of cementitious materials; although early-age strength was slightly reduced due to dilution effects, both long-term strength and durability were significantly enhanced [27]. Similarly, Bingbing Guo examined seawater sea-sand concrete subjected to CO<sub>2</sub> curing, focusing on its pore structure and uniaxial compressive behavior. The results showed that CO<sub>2</sub> curing effectively reduced mesopores and micropores, leading to a denser pore structure. After 180 days, the compressive strength increased by up to 30%; however, this was accompanied by an increase in elastic modulus and a reduction in peak strain, indicating a tendency toward enhanced brittleness [28,29]. Carbonation treatment has been demonstrated to significantly improve the performance of RCA. Antonina Goncharov et al. reported that accelerated carbonation induces reactions between CO<sub>2</sub> and calcium-bearing phases in RCA, such as calcium hydroxide and calcium silicate hydrate (C-S-H), resulting in the formation of calcium carbonate [30]. This process markedly reduces the porosity and water absorption of RCA, thereby enhancing its overall quality. In addition to achieving CO<sub>2</sub> sequestration, carbonation treatment also improves the reactivity of recycled powders in cementitious systems, reduces environmental risks, and promotes the resource utilization of solid waste [26,31]. Ding Yahong investigated the effects of accelerated carbonation under varying pressure conditions on the macro- and micro-properties of RCA. The findings indicated that with increasing carbonation pressure, the apparent density of RCA increased, while water absorption and crushing index decreased exponentially. During the carbonation process, abundant calcite crystals were deposited within pores and at interfaces, filling cracks and voids, thereby

refining the aggregate structure [32]. Further studies revealed that recycled concrete prepared with carbonated aggregates exhibited a 22.6% increase in compressive strength compared with that produced from untreated RCA. Moreover, its durability was enhanced, with a 36% improvement in resistance to external ion penetration and a 12% increase in reinforcement corrosion resistance [33–36]. These improvements can be attributed to the carbonation of major hydration products in the cement paste, such as C-S-H and Ca(OH)<sub>2</sub>, which generates calcite and highly polymerized silica gel [37]. This densification of the microstructure significantly enhances the resistance of recycled concrete to external ion ingress.

Although carbonation can enhance the performance of RCA, its effectiveness is subject to certain limitations. This is primarily because the adhered mortar on the surface of RAs is limited, and as the replacement ratio increases, the overall performance of recycled aggregate concrete (RAC) tends to decline. Kaijian Zhang et al. reported that the compressive strength of RAC decreased significantly with increasing RA content, and when the replacement level exceeded 30%, the benefits of carbonation were offset by the intrinsic defects of the aggregates[38]. Alessia Cuccurullo et al. investigated the carbonation of recycled fine aggregates under different relative humidity levels and carbonation durations, and evaluated their mechanical properties using a triaxial testing machine. The results revealed that carbonation under medium to low humidity yielded the most favorable outcomes, with a 30% replacement ratio leading to significant improvements in mechanical performance and carbonation resistance[39]. However, under high humidity or at higher replacement ratios, increased porosity and poor interfacial bonding resulted in deteriorated performance. Recycled powder, as a by-product of RA processing, is characterized by finer particle size and larger specific surface area, making it a suitable supplementary cementitious material in cement-based systems. Compared with RAs, recycled powders contain a greater amount of cement paste particles and exhibit smaller particle sizes, thereby offering superior CO<sub>2</sub> sequestration potential [41]. Carbonation treatment not only mitigates the high porosity of recycled powders but also enhances their reactivity. Ding Yahong et al. demonstrated that pre-soaking carbonation, as opposed to direct carbonation, increased the flexural strength of mortar by 27.85% and

compressive strength by 20% at a 30% replacement level, while also elevating the Ca/Si ratio, thereby facilitating a more complete hydration reaction and yielding a denser microstructure[32]. Moreover, carbonation was found to reduce the compositional heterogeneity of recycled powders, aligning their mineral phases more closely with those of Portland cement, which increased their activity index [43]. During carbonation, recycled powders can also capture a measurable amount of CO<sub>2</sub>, with studies indicating that the CO<sub>2</sub> uptake per unit of recycled fine powder is approximately 20% of the CO<sub>2</sub> emissions per unit of cement [22]. Furthermore, carbonation alters the mineral composition of recycled fine powders, and the formation of CaCO<sub>3</sub> provides additional nucleation sites for cement hydration, thereby promoting hydration processes.

In this study, scanning electron microscopy (SEM), X-ray diffraction (XRD), and nuclear magnetic resonance (NMR) techniques were employed to systematically investigate the effects of incorporating carbonated recycled fine powder on the micro-morphology, pore structure, cement hydration kinetics, and total heat evolution of cement mortars. The hydration kinetics of carbonated recycled fine powder were further examined to improve its physical and mechanical properties and to elucidate its synergistic modification effects during carbonation, thereby overcoming the limitations of conventional studies that have primarily focused on single recycled aggregates. This research not only promotes the high-value utilization of construction and demolition waste but also provides a theoretical basis for enhancing the durability of concretes containing carbonated recycled fine powder. Furthermore, it enables effective CO<sub>2</sub> sequestration, aligning with China's "dual-carbon" strategic goals.

## MATERIALS AND METHODS

### Materials

This study utilized Ordinary Portland Cement (P.O 42.5) as the binder material, conforming to the Chinese standard GB 175-2007. The recycled fine powder (RFP) was prepared from discarded concrete beams collected in the laboratory. These beams were manually broken and then subjected to secondary crushing using a universal jaw crusher. The resulting material

was sieved to obtain particles smaller than 0.16 mm, which were then placed in a ball mill and ground for 30 minutes. Following grinding, the matrix was passed through a sieve to isolate powder particles smaller than 0.075 mm. Table 1 summarizes the chemical makeup of both the RFP and the cement.

Laboratory-supplied tap water was employed for both mixing and curing. ISO standard sand was supplied by Xiamen ISO Standard Sand Co., Ltd., complying with the Chinese standard GB/T 17671.

### Carbonation treatment of RFP

The RFP was carbonated using a dry carbonation method. An accelerated carbonation chamber (Model TMS9015D, manufactured by Hangzhou Jiuwen Automation Technology Co., Ltd.) was used for the treatment. The carbonation conditions were maintained as follows: CO<sub>2</sub> concentration at 40%, temperature at 21 °C, and relative humidity at 70%. After 72 hours of carbonation, the treated powder was referred to as carbonated recycled fine powder (CRFP). Figure 1 shows the powder morphology of CRFPd and RFP.

Figure 2 presents the particle size profiles of the powders before and after carbonation. Based on laser diffraction analysis, the D<sub>50</sub> values were 9.895 µm for Portland cement, 3.892 µm for RFP, and 14.590 µm for CRFP. The RFP

exhibited a finer grain size than cement, whereas the CRFP displayed a distribution pattern closely resembling that of cement. The observed particle coarsening post-carbonation is primarily ascribed to the accumulation of reaction products on powder surfaces.

### Mix proportion design

Cement mortar specimens were prepared in accordance with GB/T 17671-2021, “Test Method for Strength of Cement Mortar (ISO Method)”, by partially replacing cement with RFP and CRFP at substitution levels of 10%, 20%, and 30% by mass. Table 2 outlines the specific mixture compositions used in this study.

### Specimen preparation

According to the designed mix proportions, cement mortar was prepared using a mortar mixer. The fresh mortar was cast into prismatic molds of 40 × 40 × 160 mm in two layers, with each layer compacted on a vibration table for a total duration of 120 s to remove entrapped air. After 24 h of curing in the molds, the specimens were demolded and subsequently cured under standard conditions. These mortar specimens were used for compressive strength and flexural strength tests. Following the same mix proportions, cylindrical mortar specimens with a diameter of 50 mm and a length of 100 mm were prepared. These

**Table 1.** Chemical composition of cementitious materials (wt.%)

| Parameter | CaO  | SiO <sub>2</sub> | Al <sub>2</sub> O <sub>3</sub> | Fe <sub>2</sub> O <sub>3</sub> | MgO   | SO <sub>3</sub> | Na <sub>2</sub> O | CO <sub>2</sub> | TiO <sub>2</sub> | K <sub>2</sub> O |
|-----------|------|------------------|--------------------------------|--------------------------------|-------|-----------------|-------------------|-----------------|------------------|------------------|
| cement    | 59.4 | 18.6             | 5.42                           | 3.81                           | 0.695 | 4.46            | 0.20              | 5.33            | 0.366            | 1.08             |
| RFP       | 19.8 | 44.9             | 10.9                           | 6.95                           | 1.63  | 0.76            | 0.901             | 10.2            | 0.856            | 2.51             |



(a) RFP

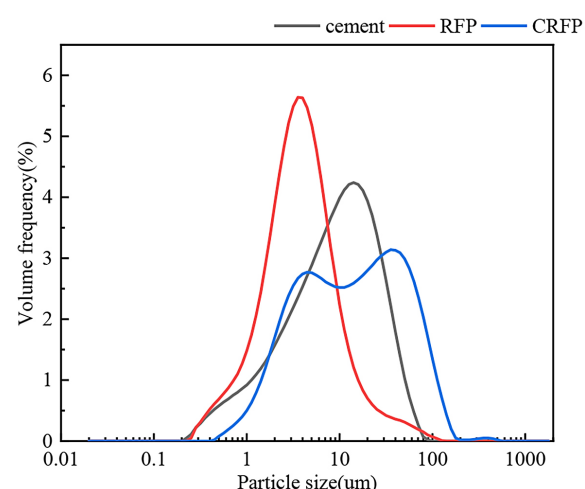


(b)CRFP

**Figure 1.** Morphology of CRFP and RFP

**Table 2.** Mix proportion design of cement mortar specimens

| Mix ID | Replacement ratio (%) | Cement/g | RFP/g | CRFP/g | Sand/g | Water/g |
|--------|-----------------------|----------|-------|--------|--------|---------|
| N-0    | 0                     | 450      | 0     | 0      | 1350   | 225     |
| C-1    | 10                    | 415      | 0     | 45     | 1350   | 225     |
| C-2    | 20                    | 360      | 0     | 90     | 1350   | 225     |
| C-3    | 30                    | 315      | 0     | 135    | 1350   | 225     |
| N-1    | 10                    | 415      | 45    | 0      | 1350   | 225     |
| N-2    | 20                    | 360      | 90    | 0      | 1350   | 225     |
| N-3    | 30                    | 315      | 135   | 0      | 1350   | 225     |

**Figure 2.** Particle size distribution of Portland cement, RFP, and CRFP

specimens were specifically designed for NMR testing to analyze the pore structure distribution within the mortar, and were not used for mechanical strength tests.

For each mix proportion, three specimens were prepared for both compressive and flexural strength testing, and three cylindrical specimens were prepared for NMR analysis. To ensure consistency, the NMR specimens were assigned the same identification numbers as the corresponding strength specimens, as they represent the pore structure characteristics of mortar with the same mix proportion. Cement mortar specimens were cured in water at  $20\pm1$  °C for 3, 7, and 28 days, while the NMR specimens were cured for

28 days. The dimensions and loading rates of the mortar specimens are summarized in Table 3.

## Testing methods

### Flexural and compressive strength testing

The mechanical performance of cement mortar specimens was evaluated following the GB/T 17671-2021 standard for cement strength determination (ISO method). Flexural strength tests were performed on a standard mortar testing device, where each sample was supported on rollers while a loading head applied force steadily at 0.05 kN/s until failure occurred. Subsequently, the two resulting halves underwent compressive strength testing at a loading rate of 2.4 kN/s. All measurements were documented and subjected to statistical analysis. The fractured pieces were then submerged in absolute ethanol to halt hydration and preserve the microstructure for later microscopic examination.

### X-ray diffraction (XRD) analysis

XRD analysis was employed to determine the phase composition and mineralogical changes in the cementitious materials. Cement mortar fragments soaked in absolute ethanol were ground into fine powder with a particle size smaller than 25 µm and then dried in an oven. The analysis was performed using a ZXS Primus X-ray fluorescence spectrometer. The scanning was conducted over a  $2\theta$  range of 5°

**Table 3.** Mix proportion design of cement mortar specimens

| Specimen type                                     | Dimensions (mm) | Loading rate (mm/min or MPa/s) | Test purpose              |
|---|-----------------|--------------------------------|---------------------------|
| Prismatic specimen                                | 40 × 40 × 16    | 50 N/s (flexural test)         | Flexural strength test    |
| Cubic specimen (halved prism after flexural test) | 40 × 40 × 40    | 2.4 kN/s (compressive test)    | Compressive strength test |
| Cylindrical specimen                              | φ50 × 100       | Not applicable (NMR only)      | Pore structure (NMR test) |

to 70°. The resulting diffraction patterns were used to identify hydration products and carbonation products.

#### *Scanning electron microscopy (SEM) analysis*

After measuring compressive strength, the fractured mortar samples were immersed in anhydrous ethanol to terminate further hydration reactions and then subjected to low-temperature drying. To improve electrical conductivity, the specimens, after drying, were coated with a thin gold layer via sputtering. Microstructural examination was performed using a JSM-6610LV scanning electron microscope (JEOL Ltd., Japan). The study primarily investigated the interfacial zones, pore distribution, and surface morphology of hydration products in cement mortar incorporating RFP and CRFP.

#### *Particle size analysis*

Particle size distribution and average diameter of cement were measured using a Winner 2000Z laser particle size analyzer, RFP, and CRFP. This assessment primarily aimed to characterize the particle size variations resulting from the carbonation process applied to RFP.

#### *Isothermal calorimetry analysis*

An I-Cal 4000 HPC isothermal calorimeter (Shanghai Rean Instrument Co., Ltd.) was utilized to examine how varying amounts of CRFP replacement affect the early hydration characteristics of cement. Monitoring the cumulative heat released and the heat release rate over the initial 72 hours allowed for assessment of the impact of CRFP dosage on hydration kinetics and the associated mechanisms.

#### *Thermogravimetric analysis (TGA)*

Thermogravimetric analysis (TGA) was conducted using a STA449 F3 simultaneous thermal analyzer (NETZSCH Instruments, Germany) to assess the thermal degradation behavior of hydration products in mortars containing RFP and CRFP. The measurements were conducted under a nitrogen atmosphere over a temperature range of 30–1100 °C, with a heating rate of 10 °C/min. This study focused on characterizing the mass loss patterns of hydration phases within various temperature intervals.

#### *Nuclear magnetic resonance (NMR) analysis*

A low-field NMR analyzer was utilized to examine how CRFP impacts the internal pore characteristics of cement mortar. This non-destructive method quantitatively evaluates porosity and pore size distribution by measuring the transverse relaxation time ( $T_2$ ) of hydrogen nuclei within pore water. By comparing samples with varying proportions of RFP and CRFP replacements, the study assessed the role of carbonation treatment in refining porous structure and altering moisture distribution inside the mortar.

## RESULTS AND DISCUSSION

### **Compressive and flexural strength of cement mortar**

Figure 4 presents the variations in flexural and compressive strengths of cement mortar incorporating different replacement ratios of RFP before and after carbonation treatment. As shown in Figure 4(a), which depicts the compressive strength, the mortar strength decreases with increasing replacement levels of RFP. Compared with the reference groups N-1, N-2, and N-3, the compressive strength of C-1, C-2, and C-3 specimens after 3 days of hydration increased by 15.2%, 14.3%, and 8.0%, respectively. At 28 days of hydration, the corresponding improvements were 4.7%, 5.2%, and 2.8%. These results indicate that the enhancement in compressive strength is more pronounced at the early hydration stage (3 days) than at the later stage (28 days). Moreover, the compressive strength improvement at lower replacement ratios (C-1 and C-2) is more pronounced than that of C-3. This can be attributed to the formation of highly reactive amorphous silica during carbonation, which reacts with  $\text{Ca}(\text{OH})_2$  to generate additional C-S-H gels at the early stage of hydration, thereby enhancing the early-age strength [43]. Ouyang Xiaowei's study further confirmed that nucleating agents such as  $\text{CaCO}_3$  and amorphous silica provide additional nucleation sites, accelerating early hydration. Finer particle sizes or higher surface activity facilitate greater adhesion of hydration products during the initial reaction stage. In addition,  $\text{CO}_2$  reacts with  $\text{Ca}(\text{OH})_2$  and other calcium-bearing phases during carbonation to form  $\text{CaCO}_3$ , which precipitates within pores and microcracks, thereby improving the compactness of the matrix. Due to the influence



(a) Compressive strength test



(b) Compressive strength test

Figure 3. Flexural and compressive strength tests of cement mortar

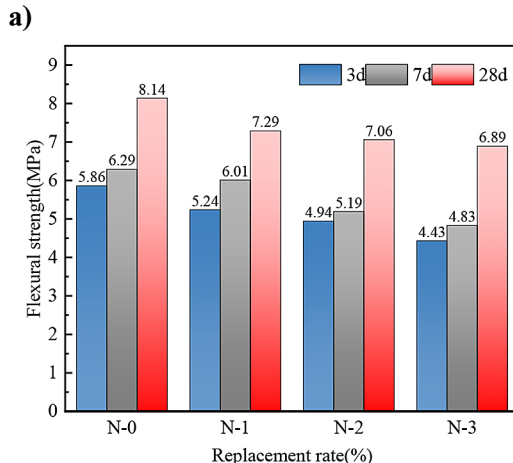
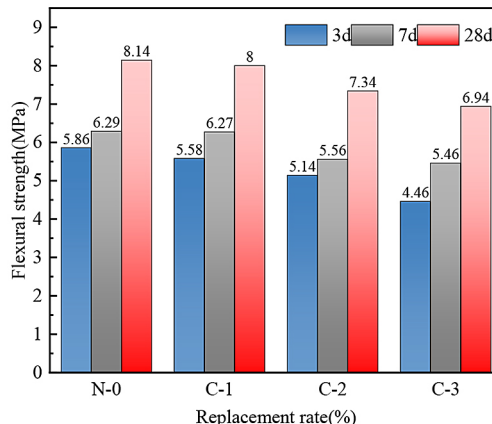
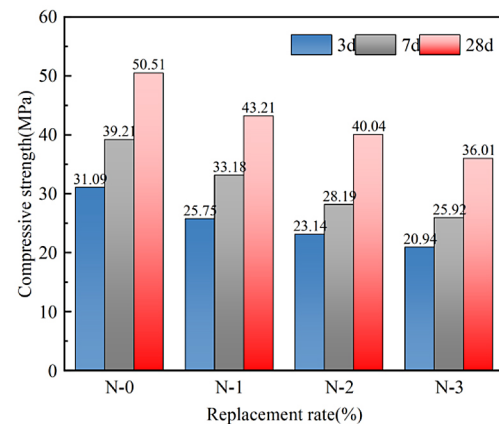
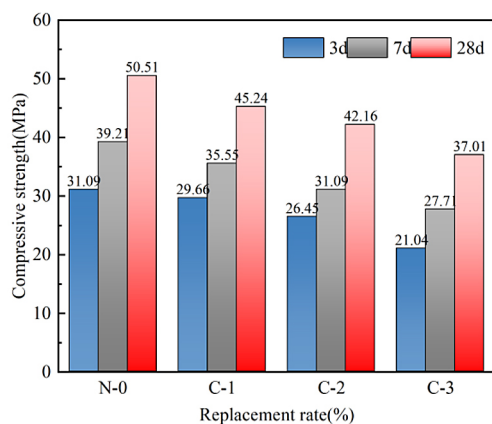


Figure 4. a) Compressive strength of cement mortars with CRFP and RFP at different replacement levels  
b) Flexural strength of cement mortars with CRFP and RFP at different replacement levels

of natural carbonation, a portion of the carbonatable hydration products in the cement matrix is consumed, thereby limiting the degree of carbonation treatment of RFP. As a result, the strength enhancement at 28 days is relatively insignificant

[27,44]. Cajun Shi pointed out that when the replacement ratio is below 20%, the strength improvement is comparable to that of the control group with 0% replacement. However, once the replacement ratio exceeds 20%, the enhancement

effect declines. The observed improvement in strength is attributed to the  $\text{CaCO}_3$  generated during carbonation, which provides abundant nucleation sites for hydration products and thereby accelerates cement hydration[45]. Similarly, the study by Ding Yahong demonstrated that at a 20% replacement ratio, carbonated CRFP can significantly improve both the strength and the activity index of mortar, with the compressive strength increased by up to 27.8% [32]. In summary, CRFP at low replacement ratios can significantly enhance the early compressive strength of cement mortar. This improvement is primarily attributed to the nucleation effect of  $\text{CaCO}_3$  and amorphous silica, which promotes the formation of hydration products and fills pores, thereby improving structural compactness. However, with increasing replacement ratios and prolonged curing ages, the strength gain gradually diminishes due to the limited extent of carbonation reactions and the consumption of carbonatable hydration products. The compressive and flexural strength results of cement mortar are presented in Figure 3.

As shown in Figure 4(b), the flexural strength of C-1, C-2, and C-3 at 3 days increased by 6.5%, 4.0%, and 0.6%, respectively, while at 28 days the corresponding increases were 9.7%, 4.0%, and 0.7%. These results indicate that carbonation enhances the bonding performance between the cement matrix and fine sand particles, leading to an interfacial transition zone enriched with hydration product coatings, thereby improving the overall structure of the mortar. Shuvo reported that carbonation treatment can activate or utilize the residual available calcium sources in recycled powder, such as  $\text{Ca(OH)}_2$  or partially reacted hydrated calcium phases. This process increases the release of  $\text{Ca}^{2+}$  at the powder–paste interface, thereby promoting the pozzolanic reaction and the formation of additional C–S–H gels, which in turn enhances the flexural performance[46]. Ding et al. investigated RFP subjected to different carbonation treatments and incorporated into mortar, and found that carbonation significantly improved the mechanical properties. Among the tested methods, pre-soaking carbonation exhibited the most pronounced effect, with flexural strength increasing by up to approximately 27.85% [47]. However, when the replacement ratio exceeded 20%, the strength enhancement gradually diminished. Zhang J. et al. investigated the role of CRFP in cement-based materials and reported that at high replacement ratios, the

strength decreases due to the dilution effect[48]. Nevertheless, the nucleation effect of  $\text{CaCO}_3$  and the optimization of pore structure can still contribute to a certain degree of strength enhancement. At low replacement ratios, CRFP can significantly enhance the flexural strength of mortar. The underlying mechanism lies in the  $\text{CaCO}_3$  and amorphous silica generated during carbonation, which act as nucleation agents within the interfacial transition zone (ITZ), promoting the formation of C–S–H gels and filling pores [35,49]. This process improves the bonding between the paste and aggregates, optimizes the pore structure, and enhances resistance to crack propagation. However, when the replacement ratio exceeds 20%, the dilution effect becomes more pronounced, and the strength gain gradually diminishes.

Analysis of mortar strength indicates that incorporating CRFP leads to improvements in both compressive and flexural strengths compared with mortar containing RFP. Carbonation transforms  $\text{Ca(OH)}_2$ , C–S–H gels, and ettringite phases present in the adhered old paste of CRFP into  $\text{CaCO}_3$  and amorphous silica, thereby densifying the microstructure [50]. The  $\text{CaCO}_3$  produced during carbonation, together with the abundant  $\text{SiO}_2$  in CRFP, provides additional nucleation sites for cement hydration, promotes the formation of hydration products, and ultimately enhances the strength of mortar containing RFP.

### Microstructural analysis

Figure 5 presents the micro-morphologies of mortars incorporating RFP at different replacement ratios (N-1, N-2, and N-3) after 3 and 28 days of hydration. As shown in the figure, cement mortar specimens incorporating RFP exhibit a relatively loose overall structure, and distinct microcracks can be observed in samples N-1, N-2, and N-3. With increasing replacement ratios, the manifestation of microcracks becomes more pronounced. This is primarily because the incorporation of RFP exerts a dilution effect on cement, which slows down the hydration process and aggravates crack development within the mortar. In contrast, although mortars containing CRFP (C-1, C-2, and C-3) also tend to exhibit a looser structure with increasing replacement ratios, their micro-morphologies remain noticeably denser compared with their uncarbonated counterparts (N-1, N-2, and N-3) at the same replacement levels. Zhu et al. reported that RFP exhibits a high water

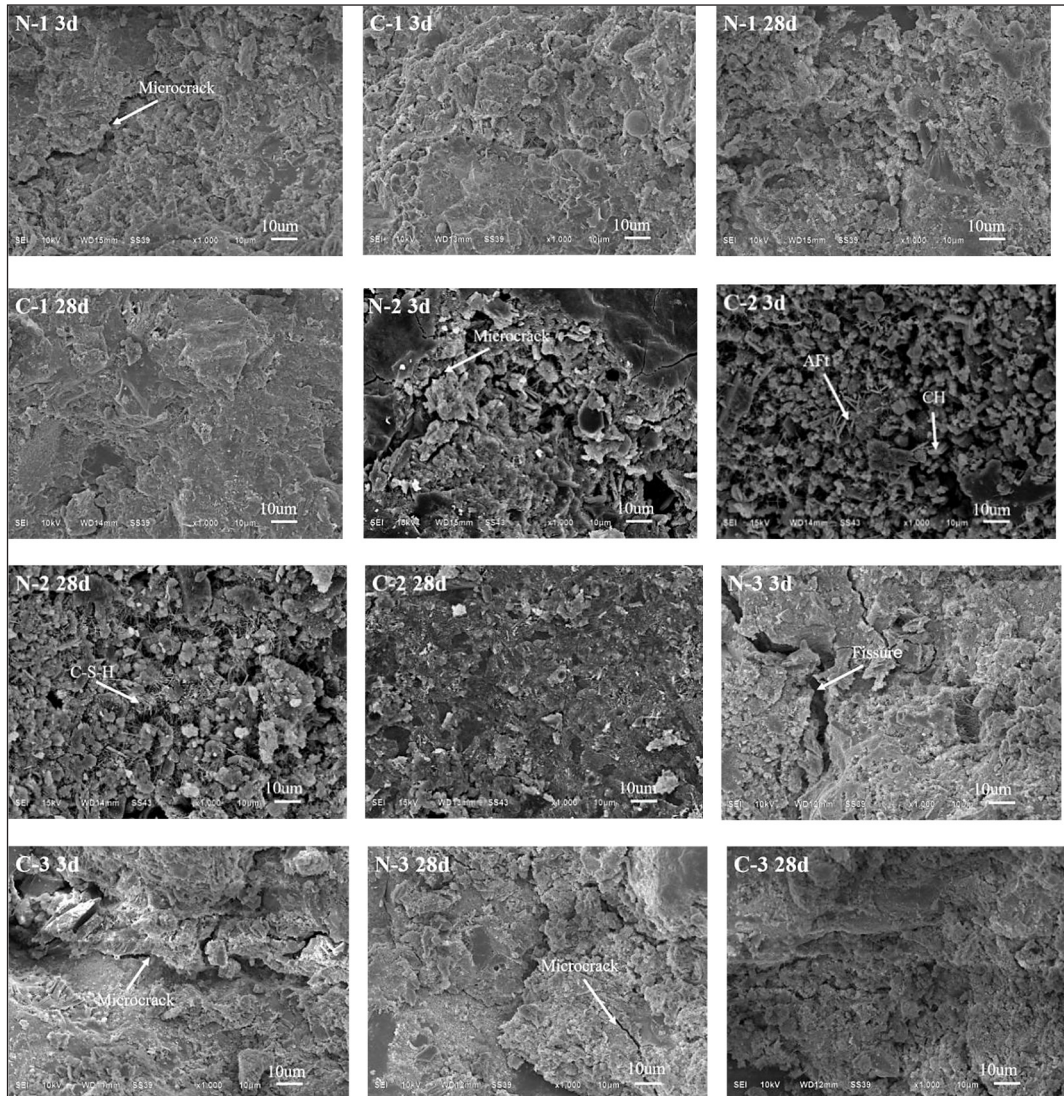


**Figure 5.** Micro-morphologies of mortar with different replacement ratios

absorption capacity, and its particle morphology and interfacial characteristics are inferior to those of cement. In RFP, the particle connections are loose, accompanied by large voids and pores. After 1 h of carbonation, however, the micro-structure tends to become denser, with abundant  $\text{CaCO}_3$  crystals and amorphous  $\text{SiO}_2$  gel formed and deposited within the pores and microcracks. This process leads to a denser interfacial transition zone (ITZ) and a stronger bonding between the colloidal products and the cement matrix [51].

The microstructures of N-1 and C-1 specimens with a 10% replacement ratio exhibited relatively high compactness after 3 and 28 days of hydration. This is because, under low replacement conditions, the system still contains a substantial amount of reactive substances, and the dilution effect of RFP on the cement hydration process is relatively minor. When the replacement ratio increased to 20%,

the C-2 specimen exhibited more flocculent and plate-like hydration products after 3 days of hydration compared with N-2. This can be attributed to the rapid nucleation and growth of early-stage C-S-H on the surface of CRFP. Ding et al. further reported that carbonated samples show a more pronounced formation of gel products during the initial hydration stage, particularly in the early to middle hydration periods. Jiang et al. further confirmed that after 3 days of hydration, specimens incorporating CRFP contained more flocculent C-S-H, ettringite, and a greater number of granular products. Compared with the uncarbonated specimens, the presence of  $\text{CO}_3^{2-}$  ions introduced by carbonation provided additional nucleation sites, which facilitated the growth of early-stage C-S-H and contributed to its more uniform distribution [32]. After 28 days of hydration, the surface structure of C-2 appeared denser than that of

N-2, indicating that carbonation can enhance the bonding performance both within the paste and between particles. This process effectively fills microcracks, resulting in a relatively compact cement mortar structure. Xiaowei Ouyang confirmed through crack characterization that CRFP particles exhibit superior performance in restraining crack propagation compared with their uncarbonated counterparts [52]. At a replacement ratio of 30%, noticeable surface cracks were observed in both N-3 and C-3 mortar specimens, regardless of whether the hydration age was 3 or 28 days. This phenomenon can be attributed to the difficulty of carbonation products in effectively filling the micro-pores under high replacement levels. Jiake Zhang pointed out that when the replacement ratio exceeds 20–30%, the excessive amount of CRFP exerts a strong dilution effect, thereby reducing the effective reactivity of cement. At high replacement levels, the availability of hydratable phases in the cement matrix decreases, and the uneven distribution of carbonation products may also lead to structural discontinuities or hinder the filling of microcracks [53].

Cement mortar incorporating RFP exhibited a relatively loose structure, with the number of microcracks increasing as the replacement ratio rose, primarily due to the dilution effect that weakened cement hydration. In contrast, CRFP generated  $\text{CaCO}_3$  crystals and  $\text{SiO}_2$ , which promoted the hydration process of cement. As a result, mortars with the same replacement ratio showed a denser structure, accompanied by faster and more uniform formation of early-stage C–S–H. Furthermore, carbonation improved the compactness of the ITZ and contributed to the filling of pores and microcracks [27,54]. At a replacement ratio of 10%, the influence on the mortar structure was relatively minor. When the replacement ratio reached 20%, the carbonated samples exhibited more abundant hydration products and a denser microstructure. However, at a 30% replacement ratio, significant cracks were observed, as the excessive dilution effect and insufficient reactivity hindered effective pore filling, thereby reducing the overall structural integrity.

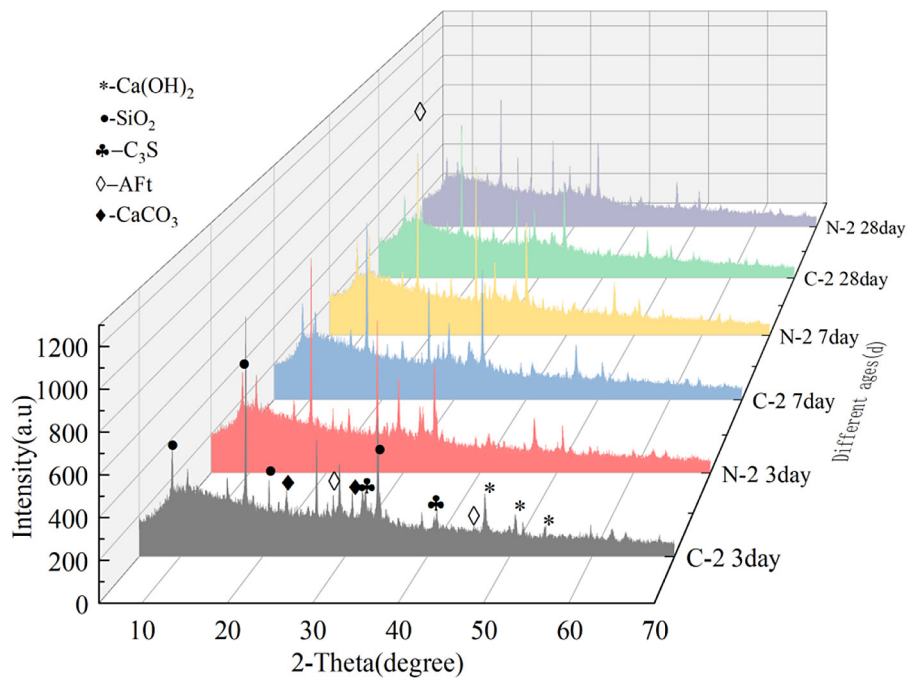
### XRD analysis

Figure 6 shows the XRD patterns of C-2 and N-2 pastes after 3, 7, and 28 days of hydration. The main crystalline phases identified include Aft,  $\text{Ca(OH)}_2$ ,  $\text{SiO}_2$ ,  $\text{C}_3\text{S}$ , and  $\text{CaCO}_3$ . It can be observed that the XRD patterns of C-2 and N-2

at different curing ages are generally similar, but differences exist in the peak intensities. A more detailed analysis reveals that at all curing ages, the  $\text{Ca(OH)}_2$  peaks of C-2 are stronger than those of N-2, whereas the  $\text{C}_3\text{S}$  peaks consistently appear weaker in C-2 than in N-2. Roz-Ud-Din Nassar reported that the weakening of  $\text{C}_3\text{S}$  peaks observed at later curing ages or with the incorporation of reactive powders indicates that CRFP promotes the hydration of  $\text{C}_3\text{S}$ . This effect is attributed to the nucleation action of carbonation products such as  $\text{CaCO}_3$  and amorphous silica, which accelerate the hydration of  $\text{C}_3\text{S}$ . Consequently, CRFP provides additional nucleation sites for cement hydration, facilitating the formation of more hydration products while simultaneously consuming greater amounts of the original cementitious phases [55]. Further analysis shows that the  $\text{CaCO}_3$  peaks of C-2 are stronger than those of N-2, and the Aft peaks exhibit a trend similar to that of  $\text{Ca(OH)}_2$ . This can be attributed to the increased presence of  $\text{CaCO}_3$  in the CRFP, which enhances the likelihood of reactions between  $\text{CaCO}_3$  and the aluminate phases [56]. With prolonged curing age, the hydration process becomes more complete, and the diffraction peaks of hydration products are further intensified. From the perspective of phase composition, carbonation significantly improves the performance of RFP. Jianzhuang Xiao suggested that carbonation treatment of RFP can effectively address the problem of compositional heterogeneity, making its phase characteristics closer to those of cement while also facilitating the transformation of its constituents [57]. Specifically, carbonation converts  $\text{Ca(OH)}_2$  and C–S–H gels in RFP into  $\text{CaCO}_3$  and amorphous silica.

### TGA analysis

As shown in Figure 7, TGA was conducted on mortar specimens with a 20% replacement ratio of RFP. During the heating process, three major weight-loss stages were observed: 80–300 °C, corresponding to the decomposition of physically bound water, C–S–H gels, and ettringite; 375–450 °C, corresponding to the decomposition of  $\text{Ca(OH)}_2$ ; and 540–950 °C, corresponding to the decomposition of  $\text{CaCO}_3$  [37]. Within the heating range of 20–1100 °C, the mass loss rate of C-2 was consistently higher than that of N-2. The total mass loss of C-2 reached 10.88%, compared with 10.23% for N-2. The greater mass loss observed



**Figure 6.** XRD patterns of mortar pastes with 20% RFP/CRFP replacement at different hydration ages

in C-2 indicates that carbonation promotes the formation of more hydration products during cement hydration. With increasing temperature, the mass loss also increased. In the range of 80–300 °C, the mass loss rate of C-2 was 3.81%, compared with 2.10% for N-2. This result is consistent with the findings of Neves Junior et al. and Zhong et al., indicating that the incorporation of CRFP leads to greater mass loss in the low- and medium-temperature ranges than uncarbonated samples. This reflects the higher total content of bound water and hydration products in the carbonated system. In the range of 375–450 °C, the mass loss rates of C-2 and N-2 were 1.40% and 1.36%, respectively. This difference can be attributed to the higher content of  $\text{Ca}(\text{OH})_2$  in C-2 undergoing thermal decomposition [42]. When the temperature rose above 540 °C, the mass loss was mainly attributed to the thermal decomposition of  $\text{CaCO}_3$ . Due to the influence of natural carbonation, the mass loss rate of  $\text{CaCO}_3$  in the N-2 sample was approximately 0.46%, whereas that of C-2 reached about 1.56%. This indicates that the carbonation process is accompanied by the formation of additional  $\text{CaCO}_3$  crystals. Consistently, previous studies have also reported greater mass loss in carbonated samples at high-temperature stages due to  $\text{CaCO}_3$  decomposition. The literature also indicates that carbonated samples generally exhibit greater mass loss in the

high-temperature range, which is a typical characteristic of  $\text{CaCO}_3$  decomposition. For example, Zhong et al. observed a similar phenomenon in their study on recycled aggregates [58]. Thermo-gravimetric analysis further demonstrates that carbonation treatment can activate the pozzolanic activity of RFP, thereby promoting the degree of cement hydration compared with RFP. This finding is consistent with the variations in product peak intensities observed in the XRD patterns.

### Heat of hydration analysis

As shown in Figure 8, the hydration heat evolution within 72 hours was measured for pastes with water-to-cement ratio of 0.5, where cement was partially replaced by CRFP and RFP at replacement ratios of 10%, 20%, and 30%. Figure 8(a) illustrates the variation in cumulative heat release of pastes with cement partially replaced by CRFP and RFP. The results show that the cumulative heat release per unit mass of cement after 72 h was 285.21 J for N-0, 253.35 J for C-1, 219.92 J for C-2, and 213.53 J for C-3. In comparison, the corresponding values for N-1, N-2, and N-3 were 255.61 J, 240.80 J, and 230.52 J, respectively. Relative to N-1, N-2, and N-3, the heat release of C-1, C-2, and C-3 increased by 0.8%, 9.5%, and 7.9%, respectively, with C-2 exhibiting the most pronounced effect in promoting cement hydration

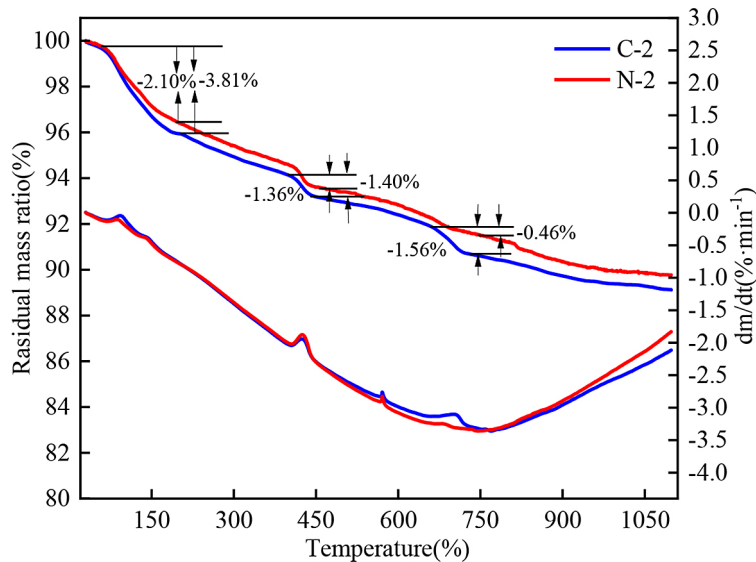


**Figure 7.** Thermogravimetric analysis of cement mortar with 20% CRFP/RCF replacement

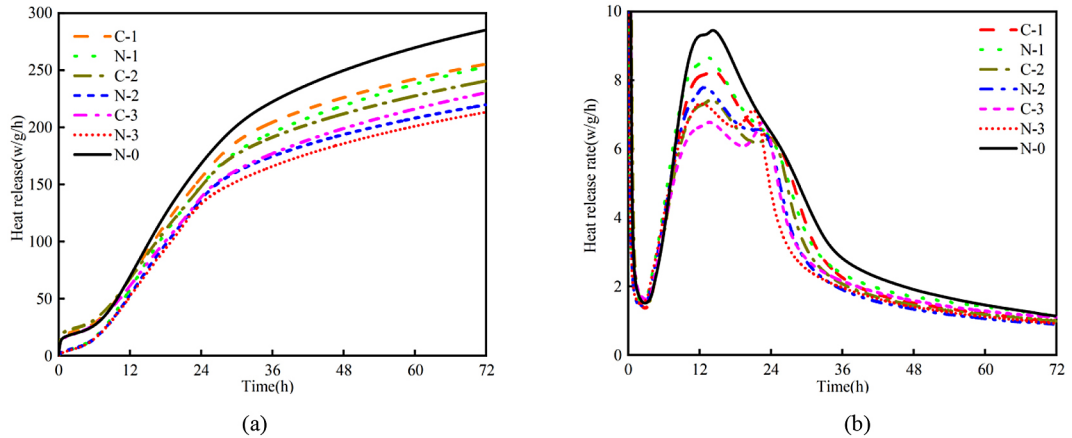
compared with C-1 and C-3. Yuanyuan Mo investigated the effect of CRFP and RFP at a 20% replacement ratio on cement hydration and found that RFP exhibited both filler and nucleation effects at the early stage. As a result, both the heat release rate and the cumulative heat release per unit mass of cement were increased [18].

Figure 8(b) shows the heat release rate curves of cement pastes with partial replacement by CRFP and RFP. The results indicate that both replacements led to noticeable changes in the hydration kinetics. In particular, the incorporation of CRFP advanced the occurrence of the first exothermic peak, while delaying the second peak. The hydration process of cement-based materials can be divided into five stages: dissolution, induction, acceleration, deceleration, and steady state [18]. Within the first 3 h of hydration, corresponding to the dissolution and induction periods, the heat release rates per unit mass of C-1, C-2, and C-3 were all higher than that of N-0. Among them, C-2 exhibited a greater heat release rate than N-0, while C-1 and C-3 showed rates similar to that of cement. In contrast, the rates of N-1, N-2, and N-3 were lower than N-0. This behavior may be attributed to the early nucleation effect of  $\text{CaCO}_3$  and the filler effect, which accelerate the reaction between  $\text{C}_3\text{A}$  and water and promote the generation of hydration products. During the acceleration period, the first exothermic peak of the RFP-incorporated samples shifted leftward, and the heat release rates per unit mass of N-1, N-2, and N-3 were consistently higher than those of

C-1, C-2, and C-3 throughout both the acceleration and deceleration periods. This phenomenon may be explained by the progressive formation of hydration products that encapsulated  $\text{C}_3\text{A}$  and cement particles, creating a physical barrier and product layer on the surfaces of  $\text{C}_3\text{A}$  and  $\text{CaCO}_3$ . In addition,  $\text{CaCO}_3$  may react with other compounds, and these reactions could consume part of the  $\text{Ca}(\text{OH})_2$ , thereby influencing the hydration kinetics of  $\text{C}_3\text{A}$  and slowing down the overall hydration process. During the deceleration period, a distinct secondary hydration peak was observed, which can be attributed to the transformation of AFt into AFm [58]. The secondary hydration peaks of N-1, N-2, and N-3 appeared earlier than those of C-1, C-2, and C-3, indicating that the incorporation of CRFP prolongs the secondary hydration of cement. Hydration heat analysis further demonstrates that CRFP promotes the early hydration of cement. Compared with RFP, CRFP increased the cumulative heat release within 72 h. However, as the hydration process progressed, the physical barrier effect and the consumption of reactive phases caused the heat release rate to decrease during the acceleration period, while the duration of secondary hydration was extended.

### NMR analysis

The  $\text{T}_2$  relaxation time is positively correlated with pore size, that is, the longer the relaxation time, the larger the corresponding pore radius. Moreover, the amplitude of the  $\text{T}_2$  signal reflects



**Figure 8.** Heat evolution rate and cumulative heat release per unit mass of cement in cement pastes with different replacement ratios of RFP

the pore size distribution: the greater the signal amplitude, the larger the number of pores [59]. NMR pore size distribution curve exhibited a bi-modal characteristic, in which the left peak (Peak 1) corresponded to mesopores and the right peak

(Peak 2) corresponded to medium-sized pores. The intensity of Peak 1 was higher than that of Peak 2, indicating that mesopores dominate the pore structure within the cement mortar. As shown in Figure 9(a), compared with N-1, N-2,

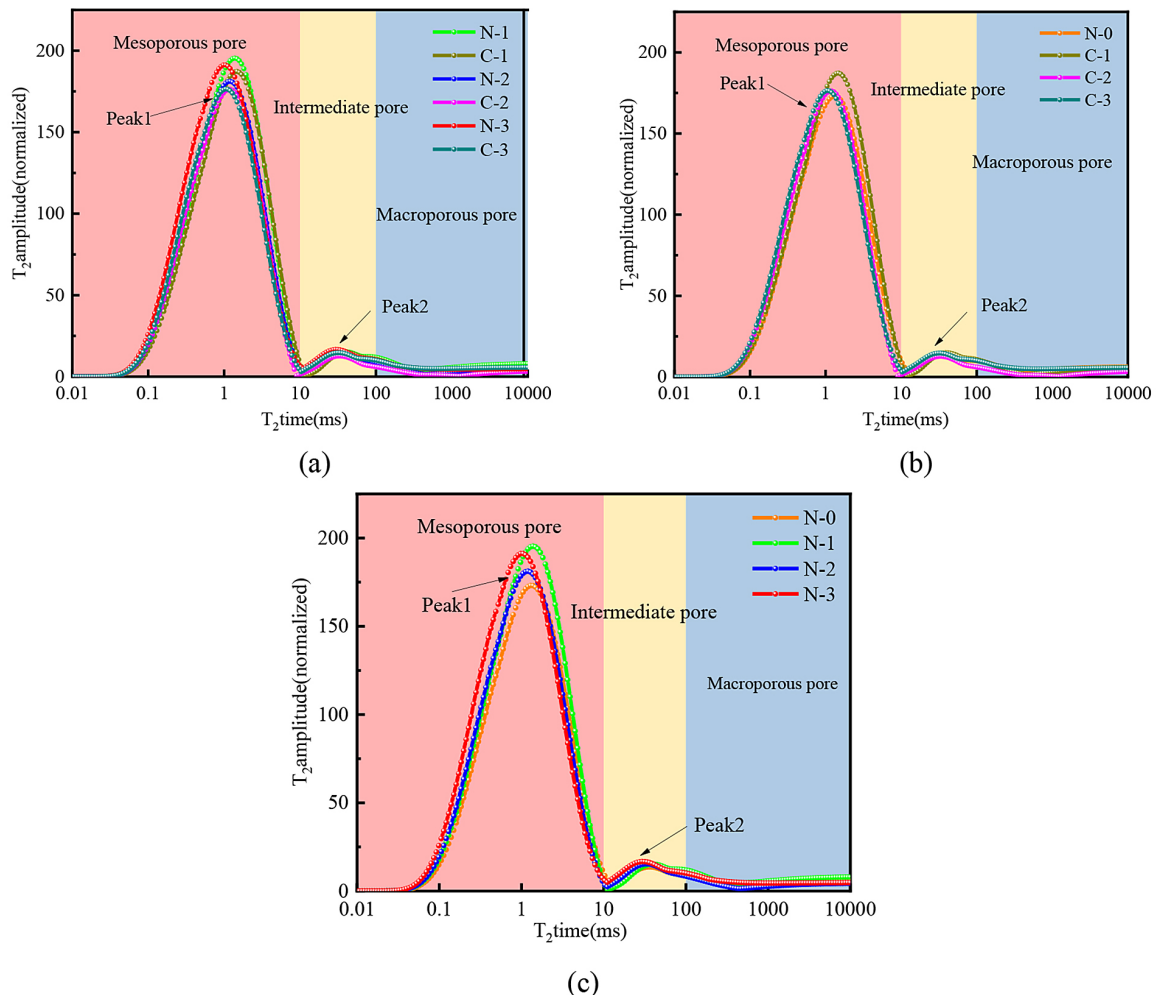


**Figure 9.** T<sub>2</sub> relaxation time distribution curves of cement mortars with RFP

and N-3, the Peak 1 profiles of C-1, C-2, and C-3 shifted rightward, while the peak intensities of both peaks were lower in C-1, C-2, and C-3. This indicates that the incorporation of CRFP increased the pore radius but reduced the overall distribution of mesopores, medium pores, and macropores [60]. As shown in Figures 9(b) and 9(c), compared with the control group N-0, both C-1, C-2, C-3 and N-1, N-2, N-3 exhibited higher values for Peak 1 and Peak 2, and the overall area of the  $T_2$  spectra was also larger. With increasing replacement ratios of CRFP and RFP, the overall curves shifted leftward, indicating that the incorporation of CRFP and RFP led to an increase in the proportion of mesopores, medium pores, and macropores in cement mortar. However, the inclusion of RFP also exerted a filling effect, resulting in an optimization of the internal pore structure. This was manifested by a reduction in the radius of mesopores as the replacement ratio increased. Roz-Ud-Din Nassar incorporated CRFP into high-performance concrete and found that, compared with RFP, the tensile strength increased by 2.96% [55]. The addition of CRFP also reduced the porosity of the specimens, thereby contributing to the improvement of concrete compactness. Based on the variations in the  $T_2$  distribution curves, it can be concluded that the incorporation of RFP increases the overall porosity of mortar. However, after carbonation treatment, the porosity of mesopores, medium pores, and macropores can be effectively reduced, although the average pore size shows a certain degree of increase.

## CONCLUSIONS

1. The incorporation of CRFP significantly improved both the mechanical properties and microstructure of cement mortar. Specifically, at low replacement ratios, compressive and flexural strengths – particularly early-age strength at 3 days – were markedly enhanced, with maximum increases exceeding 15%. The underlying mechanism is that carbonation products provide additional nucleation sites and promote the early formation of hydration products, thereby reducing porosity and improving interfacial bonding. Furthermore, thermogravimetric analysis and XRD results revealed that the CRFP group generated larger amounts of hydration products such as  $\text{Ca}(\text{OH})_2$  and  $\text{CaCO}_3$ . The heat evolution curves demonstrated that

CRFP not only accelerated early hydration but also delayed the occurrence of later hydration peaks, while pore structure analysis indicated a refinement from macropores to mesopores and medium pores. Overall, CRFP not only enhances the macroscopic mechanical performance and structural compactness of cement mortar but also contributes to mineral carbonation, offering additional environmental benefits.

2. Carbonation-treated RFP provides effective nucleation sites for cement hydration through the formation of surface carbonates and reactive  $\text{SiO}_2$ . This significantly promotes the generation of early hydration products, advances the occurrence of the first exothermic peak, and increases the total heat release, accompanied by the formation of additional  $\text{Ca}(\text{OH})_2$  and  $\text{CaCO}_3$ . Consequently, the hydration process is accelerated, and the microstructural compactness is improved.
3. Carbonated recycled aggregates primarily reduce water absorption and porosity through pore-filling effects and  $\text{CaCO}_3$  deposition, thereby improving the compactness and durability of recycled concrete. In contrast, CRFP, owing to its finer particle size and larger specific surface area, not only exhibits stronger carbon sequestration capacity but also provides abundant nucleation sites, promoting the formation of C–S–H gels, significantly enhancing early-age strength, and refining the interfacial transition zone. From both macroscopic mechanical performance and microstructural evolution perspectives, this study verifies the unique advantages of CRFP in early strength improvement and pore structure optimization, providing new theoretical foundations and practical pathways for advancing the high-value utilization of construction and demolition waste.

## Acknowledgements

I greatly appreciate the patient guidance and constructive advice provided by my supervisor, to my lab colleagues for their assistance with the experiments, and to the Laboratory of the College of Civil and Water Resources, Qinghai University, for providing essential research facilities and support.

This work was supported by the National Natural Science Foundation of China (Grant No. 51668052) and the Basic Research Program of Qinghai Province Department of Science and Technology (Grant No. 2023-ZJ-725).

## REFERENCES

1. Briki Y, Maciej Z, Haha M B, et al. (2021). Impact of limestone fineness on cement hydration at early age[J]. *Cement and Concrete Research*, 147, 106515. <https://doi.org/10.1016/j.cemconres.2021.106515>
2. Zhang Z, Angst U, Troian V, et al. (2025). Durability performance of concrete incorporating carbonated recycled coarse aggregates: A review[J]. *Materials Sustainability*, 3, 27. <https://doi.org/10.1038/s44296-025-00071-x>
3. Mao Y, Liu X, He P, Zhang J, et al. (2024). Use of carbonated recycled cement paste powder as a new supplementary cementitious material[J]. *Cement and Concrete Composites*, <https://doi.org/10.1016/j.cemconcomp.2024.3561>
4. Yang S, Gu M, Lin H, et al. (2023). Property improvement of recycled coarse aggregate by accelerated carbonation treatment under different curing conditions[J]. *Sustainability*, 15(6), 4908. <https://doi.org/10.3390/su15064908>
5. Maciej Z, Skibsted J, Skocek J, et al. (2020). Phase assemblage and microstructure of cement paste subjected to enforced, wet carbonation[J]. *Cement and Concrete Research*, 130, 105990. <https://doi.org/10.1016/j.cemconres.2020.105990>
6. Li L, Qian X, Zhao W, et al. (2023). Effect of carbonation duration on properties of recycled concrete aggregate (RCA), RCA-new mortar interface, and recycled aggregate concrete (RAC)[J]. *Journal of Cleaner Production*, <https://doi.org/10.1016/j.jclepro.2023.8203>.
7. L Wan, Yanping Zhu, Lingling Chen, et al. (2025). Effect of carbonated recycled aggregates on the mechanical properties of polymer-modified ultrathin mortar (PUM)[J]. *Journal of Engineering in Architecture and Surroundings*, <https://doi.org/10.1186/s44147-025-00609-9>
8. Zajac M, Skocek J, Durdzinski P, et al. (2020). Effect of carbonated cement paste on composite cement hydration and performance[J]. *Cement and Concrete Research*, 134, 106090. <https://doi.org/10.1016/j.cemconres.2020.106090>
9. Hu R, Zhou Y, Xing F. (2025). Strategies to improve the life cycle net CO<sub>2</sub> benefit of recycled aggregate concrete[J]. *Engineering*, <https://doi.org/10.1016/j.eng.2024.11.040>
10. Gomes HC, et al. (2025). Carbonation for enhancement of fine recycled aggregate applied to mortar[J]. *Construction and Building Materials*, <https://doi.org/10.1016/j.conbuildmat.2025.2118>
11. Jamil S, Idrees M, Akbar A, et al. (2025). Investigating the mechanical and durability properties of carbonated recycled aggregate concrete and its performance with SCMs[J]. *Buildings*, 15(2), 201. <https://doi.org/10.3390/buildings15020201>
12. Chen T, Bai M, Gao X. (2021). Carbonation curing of cement mortars incorporating carbonated fly ash for performance improvement and CO<sub>2</sub> sequestration[J]. *Journal of CO<sub>2</sub> Utilization*, 51, 101633. <https://doi.org/10.1016/j.jcou.2021.101633>
13. Wu H, Liang C, Xiao J, et al. (2021). Properties and CO<sub>2</sub>-curing enhancement of cement-based materials containing various sources of waste hardened cement paste powder[J]. *Journal of Building Engineering*, 44(2019), 102677. <https://doi.org/10.1016/j.jobe.2021.102677>
14. Mao Y, Liu X, He Pingping, et al. (2024). Use of carbonated recycled cement paste powder as a new supplementary cementitious material[J]. *Cement and Concrete Composites*, <https://doi.org/10.1016/j.cemconcomp.2024.3561>
15. Ouldkhaoua Y, Benabed B, Abousnina R, et al. (2020). Effect of using metakaolin as supplementary cementitious material and recycled CRT funnel glass as fine aggregate on the durability of green self-compacting concrete[J]. *Construction and Building Materials*, 235, 117802. <https://doi.org/10.1016/j.conbuildmat.2019.117802>
16. Kikuchi T, Kuroda Y. (2011). Carbon dioxide uptake in demolished and crushed concrete[J]. *Journal of advanced concrete technology*, 9(1), 115–124. <https://doi.org/10.3151/jact.9.115>
17. Kaddah F, Ranaivomanana H, Amiri O, et al. (2022). Accelerated carbonation of recycled concrete aggregates: investigation on the microstructure and transport properties at cement paste and mortar scales[J]. *Journal of CO<sub>2</sub> Utilization*, 57, 101885. <https://doi.org/10.1016/j.jcou.2022.101885>
18. Wang D, Xiong C, Li W, et al. (2020). Growth of calcium carbonate induced by accelerated carbonation of tricalcium silicate[J]. *ACS Sustainable Chemistry & Engineering*, 8(39), 14718–14731. <https://doi.org/10.1021/acssuschemeng.0c02260>
19. Dabiri H, Joshaghani A, Joshaghani H. (2022). Compressive strength of concrete with recycled aggregate: a machine learning-based evaluation[J]. *Cleaner Materials*, 3, 100047. <https://doi.org/10.1016/j.clema.2022.100047>
20. Wu Y, Mehdizadeh H, Mo K H, et al. (2022). High-temperature CO<sub>2</sub> for accelerating the carbonation of recycled concrete fines[J]. *Journal of Building Engineering*, 52. <https://doi.org/10.1016/j.jobe.2022.104526>
21. Torrenti J-M. (2022). The FastCarb project: taking advantage of the accelerated carbonation of recycled concrete aggregates[J]. *Journal of Cleaner Production*, <https://doi.org/10.1016/j.jclepro.2022.135716>
22. Villagrán-Zaccardi Y, Broodcoorens L, Van den Heede P, et al. (2023). Fine recycled concrete aggregates treated by means of wastewater and carbonation pretreatment[J]. *Sustainability*, 15(8), 6386.

https://doi.org/10.3390/su15086386

23. Cuccurullo A, Hou Y, Mahieux P-Y, et al. (2021). Effect of relative humidity and carbonation on the mechanical behavior of compacted fine recycled aggregates[J]. *Construction and Building Materials*, 312, 125420. https://doi.org/10.1016/j.conbuildmat.2021.125420

24. Veronica V, Federico F, Alessandro S, et al. (2023). Assessment of carbonation potential of wood ash under different curing conditions[J]. *Journal of CO<sub>2</sub> Utilization*, 69, 102346. https://doi.org/10.1016/j.jcou.2023.102346

25. Ye Y, Gu Z, Zhu C, et al. (2025). Effects of carbonation conditions and sand-to-powder ratio on compressive strength and pore fractal characteristics of recycled cement paste–sand mortar[J]. *Buildings*, 15(16), 2906. https://doi.org/10.3390/buildings15162906

26. Zhang B, Feng Y, Xie J, et al. (2023). Compressive behaviour and microstructures of concrete incorporating pretreated recycled powder/aggregates: The coupling effects of calcination and carbonization[J]. *Journal of Building Engineering*, 68. https://doi.org/10.1016/j.jobe.2023.106158

27. Lyu H, Hao L, Li L, et al. (2023). The development of sustainable cement pastes enhanced by the synergistic effects of glass powder and carbonation curing[J]. *Journal of Cleaner Production*, 418, 138237. https://doi.org/10.1016/j.jclepro.2023.138237

28. Bingbing G, Rong Y, Jinyu W, et al. (2023). Three-fold benefits of using CO<sub>2</sub> to cure seawater sea-sand concrete[J]. *Construction and Building Materials*, 401, 132868. https://doi.org/10.1016/j.conbuildmat.2023.132868

29. Jiang Y, Shen P, Poon C S. (2022 Jan.10). Improving the bonding capacity of recycled concrete aggregate by creating a reactive shell with aqueous carbonation[J]. *Construction and Building Materials*, 315. https://doi.org/10.1016/j.conbuildmat.2021.125733

30. Goncharov A, Zhutovsky S. (2022). Eco-friendly belite cement from crude calcareous oil shale with low calorific value[J]. *Cement and Concrete Research*, 159, 106874. https://doi.org/10.1016/j.cemconres.2022.106874

31. Peiris L, et al. Impact of treatment methods on recycled concrete aggregates: physical, mechanical, and durability properties[J]. *Environme*.

32. Yahong D, Ming Z, Xiaoyu Y, et al. (2024). Mechanical property and microstructure of cement mortar with carbonated recycled powder[J]. *Journal of Wuhan University of Technology—Materials Science Edition*, 39(3), 689–697. https://doi.org/10.1007/s11595-024-2927-1

33. Hanxiong L, Li H, Lei L, et al. (2023). The development of sustainable cement pastes enhanced by the synergistic effects of glass powder and carbonation curing[J]. *Journal of Cleaner Production*, 418, 138237. https://doi.org/10.1016/j.jclepro.2023.138237

34. Jean B, Kumar R, Omran A, et al. (2024). Enhancing the mechanical and durability properties of fully recycled aggregate concrete by CO<sub>2</sub>-based accelerated carbonation[J]. *Materials*, 17(9).

35. Zajac M, Skibsted J, Haha MB. (2020). Effect of alkalis on enforced carbonation of cement paste: mechanism of reaction[J]. *Journal of the American Ceramic Society*. https://doi.org/10.1111/jace.17481

36. Liu Q, et al. (2025). Performance enhancement of recycled concrete through carbonation-ready mix recycled aggregate concrete (CRRC)[J]. *Construction and Building Materials*. https://doi.org/10.1016/j.conbuildmat.2025.048074

37. Zajac M, Skibsted J, Bullerjahn F. (2022). Semi-dry carbonation of recycled concrete paste[J]. *Journal of CO<sub>2</sub> Utilization*. https://doi.org/10.1016/j.jcou.2022.102111

38. Kaijian Z, Kunjie Z, Lin W, et al. (2025). Carbonation behavior of seawater sea-sand concrete under different recycled coarse aggregate and sea-sand replacement atios[J]. *Construction and Building Materials*, 91. https://doi.org/10.1016/j.conbuildmat.2025.142592

39. Cuccurullo A, Hou Y, Mahieux P-Y, et al. (2021). Effect of relative humidity and carbonation on the mechanical behavior of compacted fine recycled aggregates[J]. *Construction and Building Materials*, 312, 125420. https://doi.org/10.1016/j.conbuildmat.2021.125420

40. Cao Y, Wang Y, Zhang Z, et al. (2021). Recent progress of utilization of activated kaolinitic clay in cementitious construction materials[J]. *Composites Part B Engineering*, 1, 108636. https://doi.org/10.1016/j.compositesb.2021.108636

41. Zhang Z, Wang Q, Zhang M, et al. (2020). A new understanding of the effect of filler minerals on the precipitation of synthetic C–S–H[J]. *Journal of Materials Science*, 55(35), 16455–16469. https://doi.org/10.1007/s10853-020-05185-2

42. Matos PRD, Sakata RD, Ong hero L, et al. (2021). Utilization of ceramic tile demolition waste as supplementary cementitious material: An early-age investigation[J]. *Journal of Building Engineering*, 102187. https://doi.org/10.1016/j.jobe.2021.102187

43. Yuan C, Wang D, Setiawan H, et al. (2021). Effect and mechanism of different excitation modes on the activities of the recycled brick micro-powder[J]. *Science and Engineering of Composite Materials*, 28(1), 676-688. https://doi.org/10.1515/secm-2021-0062

44. Xiaowei O, Liquan W, Shida X, et al. (2020). Surface characterization of carbonated recycled concrete fines and its effect on the rheology, hydration

and strength development of cement paste[J]. *Cement & Concrete Composites*, 116: 103787. <https://doi.org/10.1016/j.cemconcomp.2020.103787>

45. Mao Y, He P, Drissi S, Shi C, et al. (2024). Effect of wet carbonated recycled cement paste powder on the rheology of cement paste[J]. *Cement and Concrete Research*, 181, 107553. <https://doi.org/10.1016/j.cemconres.2024.107553>

46. Shuvo AK, Sarker PK, Shaikh FUA, et al. (2025). Enhancement of attached mortar in recycled aggregates of returned concrete by wet carbonation. *Journal of Materials in Civil Engineering*.

47. Jiake Z, Liupeng Z, Boyang X, et al. (2023). Influences of carbonated recycled concrete fines on cement hydration[J]. *Buildings*, 13(4), 926. <https://doi.org/10.3390/buildings13040926>

48. Feng Y, Li J, Zhang B, et al. (2023 Sep.15). Concrete improvement incorporating recycled powder and aggregates treated via a combination of calcination and carbonation: The impact behaviors[J]. *Journal of cleaner production*, 418. <https://doi.org/10.1016/j.jclepro.2023.138069>

49. A X F, A D X, B B Z, et al. (2020). A novel upcycling technique of recycled cement paste powder by a two-step carbonation process - ScienceDirect[J]. *Journal of Cleaner Production*.

50. Mehdizadeh H, Ling TC, Cheng X, et al. (2021). CO<sub>2</sub> Treatment of hydrated cement powder: characterization and application consideration[J]. *Journal of Materials in Civil Engineering*, 4, 33. [https://doi.org/10.1061/\(ASCE\)MT.1943-5533.0003652](https://doi.org/10.1061/(ASCE)MT.1943-5533.0003652)

51. Zhu CH, Fang Y, Wei H. (2018). Carbonation-cementation of recycled hardened cement paste powder [J]. *Construction and Building Materials*, 192, 224–232. <https://doi.org/10.1016/j.conbuildmat.2018.10.113>

52. Habert G, Miller S A, John VM, et al. (2020). Environmental impacts and decarbonization strategies in the cement and concrete industries[J]. *Nature Reviews Earth & Environment*, 1(11). <https://doi.org/10.1038/s43017-020-0093-3>

53. Cuccurullo A, Hou Y, Ma HP-Y, et al. (2021). Effect of relative humidity and carbonation on the mechanical behavior of compacted fine recycled aggregates[J]. *Construction and Building Materials*, 312, 125420. <https://doi.org/10.1016/j.conbuildmat.2021.125420>

54. Mao Y, He P, Drissi S, et al. (2023). Effect of conditions on wet carbonation products of recycled cement paste powder[J]. *Cement and Concrete Composites*, 144, 105307. <https://doi.org/10.1016/j.cemconcomp.2023.105307>

55. Nassar R-U-D, Zaid O, Elhadi KM. (2024). Utilizing carbonated recycled concrete fines to develop sustainable ultra-high-performance fiber-reinforced concrete [J]. *Journal of Building Engineering*, 99, 111634. <https://doi.org/10.1016/j.jobe.2024.111634>

56. Yang J, Piao R, Zhu C, et al. (2024). Carbonation mechanism and cementation properties of recycled cement paste based on CO<sub>2</sub> injection time and pressure [J]. *Construction and Building Materials*, 447, 138104. <https://doi.org/10.1016/j.conbuildmat.2024.138104>

57. Tang Y, Xiao J, Wang D, et al. (2023). Effect of carbonation treatment on fracture behavior of low-carbon mortar with recycled sand and recycled powder [J]. *Cement and Concrete Composites*, 142, 105178. <https://doi.org/10.1016/j.cemconcomp.2023.105178>

58. Zhong W, Wang P, Ye N, Shu K, et al. (2025). Effects of different carbonation treatment methods for recycled concrete aggregate [J]. *Buildings*, 15(17), 3054. <https://doi.org/10.3390/buildings15173054>

59. Cheng S, Liang Q, Chen G, et al. (2025). Study on the effect of carbonated recycled coarse aggregate admixture on the properties of self-compacting concrete [J]. *Waste and Biomass Valorization*, *in press*. <https://doi.org/10.1007/s12649-025-03087-7>

60. Zhang J, Zhang L, Xu B, et al. (2023). Influences of carbonated recycled concrete fines on cement hydration [J]. *Buildings*, 13(4), 926. <https://doi.org/10.3390/buildings13040926>